Available online at www.sciencedirect.com
ScienceDirect
Ceramics International 37 (2011) 3509–3514
CERAMICS INTERNATIONAL
www.elsevier.com/locate/ceramint

Effect of Zr/Ti ratio on piezoelectric properties of $Pb(Ni_{1/3}Sb_{2/3})O_3$–$Pb(ZrTi)O_3$ ceramics

C.M. Lonkar [a,*], D.K. Kharat [a], H.H. Kumar [a], Sahab Prasad [b], Mrinal Ghosh [c], C.S. Kumbhar [d]

[a] *PZT Centre, Armament R&D Establishment, Pune, India*
[b] *Defence Institute of Advanced Technology, Pune, India*
[c] *High Energy Materials Research Laboratory, Pune, India*
[d] *Naval Materials Research Laboratory, Mumbai, India*

Received 26 April 2011; received in revised form 26 May 2011; accepted 3 June 2011
Available online 12 June 2011

Abstract

Piezoceramic compositions $[Pb(Ni_{1/3}Sb_{2/3})]_{0.02}$–$[Pb(Zr_{1-y}Ti_y)]_{0.98}O_3$ with $y = 0.46$–0.50 were synthesized by solid state route to study the effect of Zr/Ti ratio on crystal structure, microstructure, piezoelectric and dielectric properties. Calcination was performed at 1060 °C. The specimens were sintered at 1280 °C for 1 h. X-ray diffraction studies indicate the co-existence of tetragonal and rhombohedral perovskite phases in these compositions. Microstructural analysis showed the dense and uniform microstructure for $[Pb(Ni_{1/3}Sb_{2/3})]_{0.02}$–$[Pb(Zr_{0.52}Ti_{0.48})]_{0.98}O_3$. This composition was resulted in optimum values of properties viz. charge constant ($d_{33} = 301 \times 10^{-12}$ C/N), voltage constant ($g_{33} = 33.7 \times 10^{-3}$ V m/N), product of piezoelectric charge constant and voltage constant ($d_{33} \times g_{33} = 10.12 \times 10^{-12}$ C V m/N^2) and coupling factor ($k_p = 0.63$). Results indicated that this material composition could be suitable for power harvesting and sensor applications.

Keywords: Power harvesting materials; High g_{33} piezoceramic; Piezoelectric materials; PNS–PZT

1. Introduction

Lead zirconate titanate (PZT) based piezoceramics are of technological interest to design various sensors and actuators as they offer excellent piezoelectric properties [1]. Optimum piezoelectric properties can be obtained when Zr/Ti ratio is about 52/48 which corresponds to the composition of the ferroelectric morphotropic phase boundary (MPB) separating the ferroelectric tetragonal (F_T) and ferroelectric rhombohedral (F_R) phases [2]. Since PZT based piezoelectric ceramics are excellent electromechanical energy converters, they can produce electrical output in response to ambient energy, vibrations, movements, etc. [3]. It could be stored and subsequently used for operation of low electric power devices. This can offer the solution to the ‘limited battery life’ problem of the modern low power devices like embedded structural health monitoring system (SHM), micro-electro mechanical systems (MEMS), etc. where the replacing of exhausted battery is very expensive or impossible some times under very specific conditions [4].

The electrical output obtained from piezoceramics is determined mainly by the product of piezoelectric charge constant and voltage constant ($d_{33} \times g_{33}$). A material with higher $d_{33} \times g_{33}$ and higher g_{33} offers higher output hence is the essential criteria for the material intended to be use for energy harvesting applications [5–8]. This condition is satisfied when piezoelectric charge constant (d_{33}) and voltage constant (g_{33}) are on higher side and dielectric constant (K_3^T) is on lower side. Since, electromechanical coupling factor (k_p) represents the energy conversion efficiency of the material, its higher value is preferred. Moreover, higher the piezoelectric voltage constant (g_{33}), higher is the sensitivity of the material making it suitable for sensor application [9].

$[PbNiSb]_x$–$[Pb(Zr_{1-y}Ti_y)]_{1-x}O_3$ is a ternary solid solution abbreviated as PNS–PZ–PT. It has been studied by some of the researchers around the MPB of PNS–PZ–PT (i.e. 0.12 PNS–0.40 PZ–0.48 PT). Zahi et al. studied the composition with general chemical formula xPZ–$(90 - x)$PT–10PNS where x lies

* Corresponding author. Tel.: +91 9822495090.
E-mail addresses: cmlonkar@hotmail.com, cmlonkar@gmail.com (C.M. Lonkar).

0272-8842/$36.00 © 2011 Elsevier Ltd and Techna Group S.r.l. All rights reserved.
doi:10.1016/j.ceramint.2011.06.006

between 39 and 47 mol%. They investigated the properties dielectric constant (K_3^T), coupling factor (k_p) and curie temperature (T_c) for the components sintered at 1180 °C for 2 h. Optimum $K_3^T = 3100$ and $k_p = 0.69$ were reported for the composition 0.10 PNS–0.44 PZ–0.46 PT in which F_T and F_R co-exist. Curie temperature was reported with rising trend from 250 °C to 305 °C as Zr/Ti ratio was decreased from 46/44 to 41/49 at 10 mol% of PNS [10]. Yu and Hsieh investigated the effect of MnO_2 (0.0–0.2 wt%) in 0.12PNS–0.40PZ–0.48PT system on properties viz. K_3^T, k_p, mechanical quality factor (Q_m) and dielectric loss factor (tan δ). Dense microstructure having grain size 7.8 μm was reported for 0.15 wt% addition of MnO_2. Properties reported for this composition were $K_3^T = 3069$, $k_p = 0.68$, $Q_m = 181$ and tan $\delta \sim 0.05$ [11]. Wang studied the compositions xPNS(52 − x)PZ–48PT for x from 2 to 14 mol% and compositions 12PNS–(88 − y)PZ–yPT, where y ranging from 44 to 52 mol%. The properties studied by them were density, k_p and Q_m. They reported maximum k_p (=0.488) and minimum Q_m (=292.5) for the composition 12PNS–40PZ–48PT sintered at 1280 °C for 2 h [12].

In the above studies d_{33} and g_{33} parameters were not reported. Moreover, K_3^T obtained by Zahi et al. and Yu and Hsieh was on higher side (∼3000+) attributing to lowering g_{33} and $d_{33} \times g_{33}$, making material less suitable for power harvesting application.

The objective of the present work was to study the effect of Zr/Ti ratio on structural, piezoelectric and dielectric properties of composition $[Pb(Ni_{1/3}Sb_{2/3})]_{0.02}–[Pb(Zr_{1-y}Ti_y)]_{0.98}O_3$ with $y = 0.46–0.50$ and its optimization for higher values of piezoelectric charge constant (d_{33}), piezoelectric voltage constant (g_{33}), product of piezoelectric charge constant and voltage constant ($d_{33} \times g_{33}$), and electromechanical coupling factor (k_p) so that it could be suitable for power harvesting applications.

2. Experimental

The compositions $[Pb(Ni_{1/3}Sb_{2/3})]_{0.02}–[Pb(Zr_{1-y}Ti_y)]_{0.98}O_3$ (hereafter abbreviated as PNS–PZT) with $y = 0.46–0.50$ were synthesized using the oxides of elements in the powder form. The raw materials used were PbO (De Waldies Ltd., Kolkata, 99.5%), ZrO_2 (Loba Chemie, 99.37%), TiO_2 (Travancore Titanium Products, 98.5%), NiO (Acros, 97%), Sb_2O_5 (Loba Chemie, 99%). The compositions were prepared and processed through mixed oxide route. Powders were wet milled for 24 h in pure water medium and zirconia balls were used as grinding media. Solid state reaction was carried out at 1060 °C and further powder was ultra-fine ground to 1.0–1.2 μm. The compositional effect on crystal structure was studied from X-ray diffraction (XRD) patterns recorded for position 2θ from 20° to 70° by Philips X'pert Pro. The powder was pressed by semi-automatic die punch machine to form discs of Ø17.2 mm × 1.7 mm thickness. The specimens were sintered at 1280 °C for 1 h. Sintered specimens were lapped and subsequently electroded with silver paste. Poling was performed at DC field of 35 kV/cm at 100 °C for 30 min. Specimens were aged for 10 days and then characterized for piezoelectric and dielectric properties like capacitance (C), tan δ, impedance (Z_m), resonance frequency (f_r) and anti-resonance frequency (f_a) using variable frequency LCR meter (Hioki Hi Tester model 3532 and 3522). Piezoelectric charge constant (d_{33}) was measured using d_{33} Berlincourt meter (CPDT 3330). The following standard empirical relations were used to calculate K_3^T, g_{33} and k_p and Q_m [12–14].

$$K_3^T = \frac{Ct}{\varepsilon_0 A} \tag{1}$$

$$g_{33} = \frac{d_{33}}{K_3^T \varepsilon_0} \tag{2}$$

$$k_p = \sqrt{2.51 \frac{f_a - f_r}{f_r}} \tag{3}$$

$$Q_m = \frac{1}{2\pi f_r Z_m C}\left(\frac{f_a^2}{f_a^2 - f_r^2}\right) \tag{4}$$

where K_3^T is the dielectric constant; C the capacitance (F); ε_0 the permittivity of free space (8.854×10^{-12} F/m); t the thickness of specimen (m); A the area of specimen (m^2); g_{33} the piezoelectric voltage constant (V m/N); d_{33} the piezoelectric charge constant (C/N); f_r the resonance frequency (kHz) and f_a is the anti-resonance frequency (kHz).

Samples were prepared for microstructure analysis by chemically etching the *polished* surface. Microstructural analysis was carried out by Scanning Electron Microscope Made – FEI Netherlands (model – Quanta 200 ESEM).

3. Results and discussion

3.1. Structural characterization

X-ray diffraction patterns of calcined powder are shown in Fig. 1 for the compositions $[Pb(Ni_{1/3}Sb_{2/3})]_{0.02}–[Pb(Zr_{1-y}Ti_y)]_{0.98}O_3$ with $y = 0.46–0.50$, i.e. the Zr/Ti ratio is reduced from 54/46 to 50/50. XRD patterns show the polycrystalline nature. Intense peak for (1 1 0) plane indicates

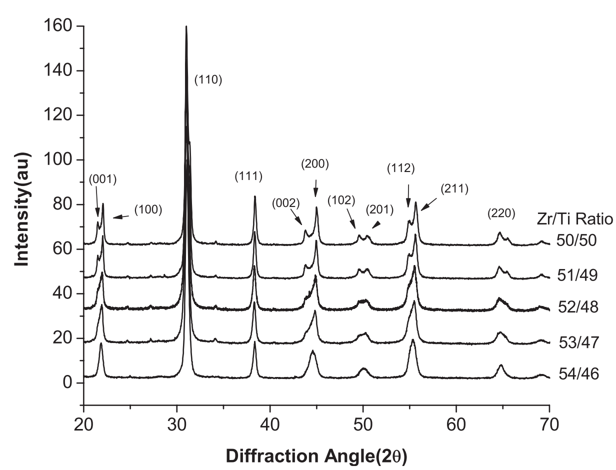

Fig. 1. XRD patterns by compositions with variation in Zr/Ti ratio.

the formation of perovskite phase for all compositions [15]. The splitting in the peak intensity at triplet (0 0 2), (1 0 2) and (1 1 2) indicate the presence of both ferroelectric tetragonal (F_T) and ferroelectric rhombohedral (F_R) phases [12,16–18]. When Zr/Ti ratio was reduced, the splitting of peak intensity at (0 0 2), (1 0 2) and (1 1 2) was predominant, indicating the increase in tetragonality which was confirmed from the calculations of *c*/*a* ratio from XRD data (Table 1). It was also observed that reduction in Zr/Ti ratio, reduced the unit cell parameter '*a*' and increased '*c*'. This has net effect on

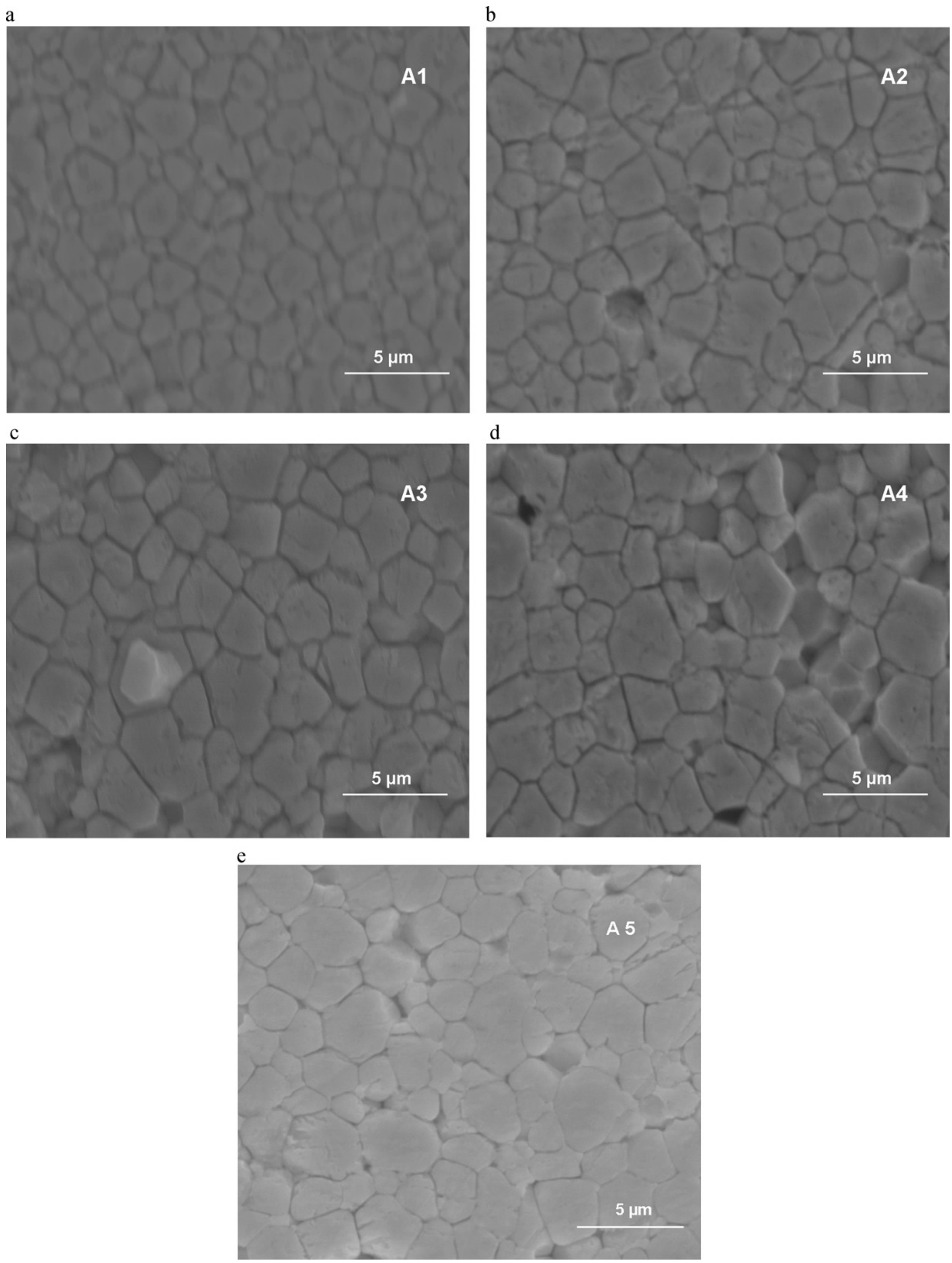

Fig. 2. (a) Zr/Ti ratio 54/46, (b) Zr/Ti ratio 53/47, (c) Zr/Ti ratio 52/48, (d) Zr/Ti ratio 51/49 and (e) Zr/Ti ratio 50/50.

Table 1
Zr/Ti ratio and tetragonal unit cell parameters.

Zr/Ti	*a* (Å)	*c* (Å)	*c/a*
54/46	4.0428	4.1127	1.0173
53/47	4.0388	4.1173	1.0194
52/48	4.0357	4.121	1.0211
51/49	4.0313	4.1267	1.0237
50/50	4.0278	4.1288	1.0251

increasing the *c/a* ratio and thus the tetragonality. This demonstrates the transformation $F_R \rightarrow F_T$.

3.2. Micro-structural analysis

Fig. 2a–e represents the effect of Zr/Ti ratio on microstructure of PNS–PZT. For Zr/Ti ratio 54/46 (Fig. 2a), the grain size is distributed widely up to 2 μm. The average grain size was about 1.4 μm. The grain size was measured by linear intercept method. Some pores were also seen. Polycrystalline piezoceramic materials are generally composed of grains, grain boundaries and pores. Presence of pores retards the grain growth [11]. For Zr/Ti ratio 53/47 (Fig. 2b) the grain size was seen to be increased as porosity was reduced; size distribution was also narrowed down in comparison with earlier one. The average grain size was about 1.6 μm. In case of Zr/Ti ratio 52/48, the grains were slightly increased in size (Fig. 2c). Grain size distribution was still narrowed down and uniform and dense microstructure was seen. Most of the grains were polygonal in shape. Few pores were seen. The average grain size measured was about 1.85 μm. Electromechanical properties were greatly influenced by grain size [19]. Dense microstructure with optimum grain size resulted in better piezoelectric properties [20]. On further reducing the Zr/Ti ratio to 51/49, average grain size was increased to 2.4 μm (Fig. 2d). Uniformity in the grain structure was reduced and grain size distribution was broadened. Further reducing the Zr/Ti ratio to 50/50 average grain size increased slightly (Fig. 2e). The average grain size was about 2.45 μm. Broad grain size distribution is seen. Porosity was also increased. Over all, it was observed that the grain growth was promoted as the Zr/Ti ratio was reduced. For Zr/Ti ratio 52/48, dense and uniform microstructure with minimum porosity was seen.

3.3. Effect of Zr/Ti ratio on properties

Fig. 3 shows the effect of Zr/Ti ratio on mechanical quality factor (Q_m) and electro-mechanical coupling factor (k_p). As the ratio was reduced from 54/46 to 52/48, Q_m reduced from 176 to 162. This indicates the increase in domain wall movement as Zr/Ti was reduced. Q_m (=162) was minimum for Zr/Ti ratio 52/48. As the ratio was further reduced, Q_m increased to 176 for Zr/Ti ratio 50/50. On the other hand k_p was increased from 0.43 to 0.52 as the ratio was reduced from 54/46 to 53/47 indicating the increasing polarisability of the material. k_p (=0.63) was maximum for Zr/Ti equals 52/48. On further reducing it, k_p was decreased to 0.39 at Zr/Ti ratio was 50/50. Since, k_p alone can indicate the strength of poling, it was concluded that the composition $[Pb(Ni_{1/3}Sb_{2/3})]_{0.02}$–$[Pb(Zr_{1-y}Ti_y)]_{0.98}O_3$ has maximum polarisability when Zr/Ti ratio was 52/48 at which dense and uniform microstructure was obtained. Maximum polarisability has resulted into minimum Q_m and maximum k_p.

Fig. 4 shows the effect of Zr/Ti ratio on dielectric properties. It is seen that on reducing Zr/Ti ratio, the dielectric constant (K_3^T) was increased and the dielectric losses (i.e. tan δ) were reduced. As the Zr/Ti ratio was decreased, *c/a* ratio was increased (Table 1) attributing to increase in K_3^T. K_3^T was increased from 774 to 1215 as Zr/Ti ratio was reduced from 54/46 to 50/50. It indicates that as Zr/Ti ratio was reduced, the charge storing capacity was increased for PNS–PZT. Friction between the domain walls, represented by tan δ, has shown deceasing trend with decreasing the Zr/Ti ratio. tan δ was reduced from 0.017 to 0.008 as Zr/Ti ratio was reduced from 54/46 to 50/50.

Fig. 5 shows the effect of Zr/Ti ratio on piezoelectric charge constant (d_{33}) and piezoelectric voltage constant (g_{33}). With the decrease in the Zr/Ti ratio, both d_{33} and g_{33} initially increase till the Zr/Ti ratio was 52/48. At this ratio optimum value of d_{33} (301×10^{-12} C/N) was obtained. This was attributed to the reduction in the porosity. The presences of pores decrease the polarization per unit volume [12] which was leading to decrease in d_{33}. On further decreasing the Zr/Ti ratio to 50/50 in steps, d_{33} was decreased attributed to the increase in porosity.

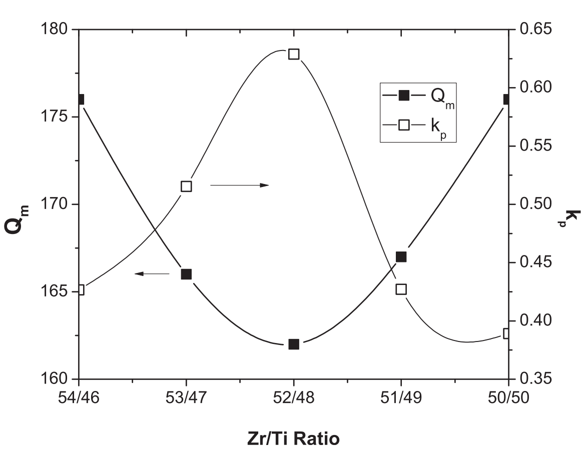

Fig. 3. Effect of Zr/Ti ratio on Q_m and k_p.

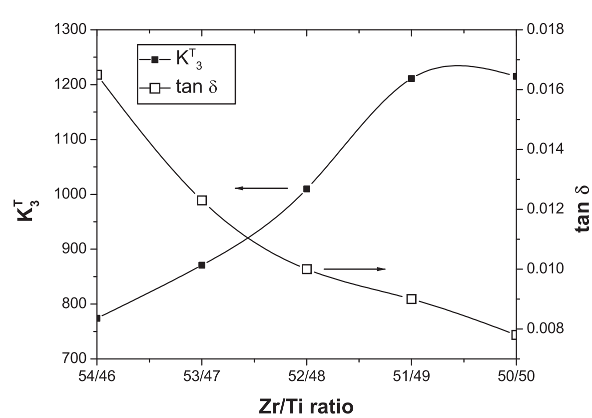

Fig. 4. Effect of Zr/Ti ratio on K_3^T and tan δ.

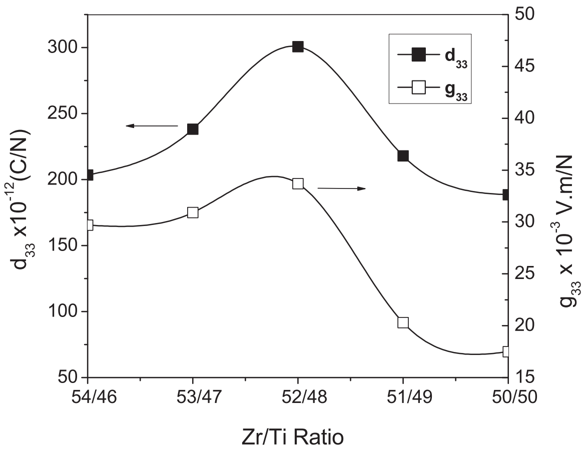

Fig. 5. Effect of Zr/Ti ratio on d_{33} and g_{33}.

As indicated by Eq. (2), g_{33} is directly proportional to d_{33} and was optimum (33.7×10^{-3} V m/N) for this ratio. This indicates that material has higher voltage producing ability and higher sensitivity for Zr/Ti ratio 52/48.

Fig. 6 shows the effect of Zr/Ti ratio on product $d_{33} \times g_{33}$. The electrical output of the material when it is used in the transducer design is highly influenced by this parameter. With the decrease in the Zr/Ti ratio, this product increased almost linearly from $6.05 \times 12 \times 10^{-12}$ C V m/N^2 to 10.12×10^{-12} C V m/N^2 till the ratio approaches 52/48. Since both, d_{33} and g_{33} were optimum for Zr/Ti ratio 52/48, obliviously the product $d_{33} \times g_{33}$ was also optimum for the same ratio. On further reducing the ratio to 50/50 in steps, this parameter reduced drastically to 3.30×10^{-12} C V m/N^2.

3.4. Effect of PNS on properties

The PZT composition and its variants have been widely studied by many researchers. Comparison of properties of basic composition $Pb(Zr_{0.52}Ti_{0.48})O_3$ and 2 mol% of PNS in basic composition $Pb(Zr_{0.52}Ti_{0.48})O_3$ is given in Table 2. It is seen that by addition of PNS, d_{33} increased from 223×10^{-12} C/N to 301×10^{-12} C/N and tan δ from 0.004 to 0.01. Reduction in

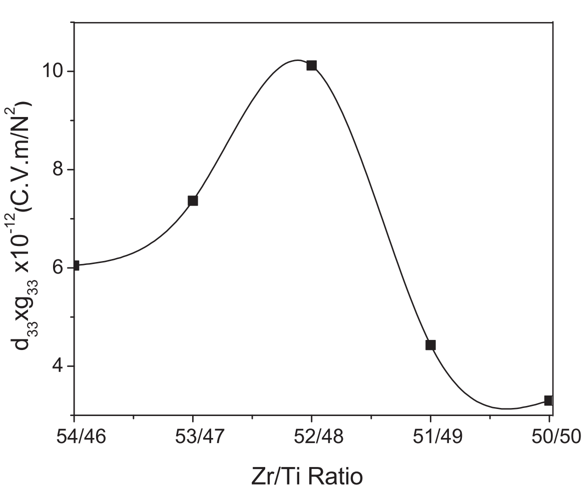

Fig. 6. Effect of Zr/Ti ratio on $d_{33} \times g_{33}$.

Table 2
Comparison of property of composition $Pb(Zr_{0.52}Ti_{0.48})O_3$ and $[Pb(Ni_{1/3}Sb_{2/3})]_{0.02}$–$[Pb(Zr_{0.52}Ti_{0.48})]_{0.98}O_3$.

Property	$Pb(Zr_{0.52}Ti_{0.48})O_3$ [2, p. 146]	$[Pb(Ni_{1/3}Sb_{2/3})]_{0.02}$–$[Pb(Zr_{0.52}Ti_{0.48})]_{0.98}O_3$ (composition under study)
Q_m	500	162
k_p	0.52	0.63
K_3^T	1180	1010
tan δ	0.004	0.01
$d_{33} \times 10^{-12}$ C/N	223	301
$g_{33} \times 10^{-3}$ V m/N	21.34	33.7
$(d_{33} \times g_{33}) \times 10^{-12}$ V m C/N^2	4.76	10.12

Q_m from 500 to 162 was also observed. However k_p, g_{33} and $d_{33} \times g_{33}$ were improved drastically due to presence of 2 mol% of PNS.

4. Conclusions

Piezoceramic composition $[Pb(Ni_{1/3}Sb_{2/3})]_{0.02}$–$[Pb(Zr_{1-y}Ti_y)]_{0.98}O_3$, where $y = 0.46$–0.50 has been studied. Presence of 2 mol% of PNS in PZT at MPB increases the domain wall movement and polarisability. In $[Pb(Ni_{1/3}Sb_{2/3})]_{0.02}$–$[Pb(Zr_{1-y}Ti_y)]_{0.98}O_3$ system, on reducing the Zr/Ti ratio, *c*/*a* ratio of tetragonal unit cell increased which resulted in improvement in dielectric constant. Dense and uniform microstructure was obtained for the PNS–PZT composition at Zr/Ti = 52/48 which resulted in optimum d_{33} (301×10^{-12} C/N), g_{33} (33.7×10^{-3} V m/N), $d_{33} \times g_{33}$ (12.1×10^{-12} C V m/N^2) and k_p (0.63). The power harvesting capability ($d_{33} \times g_{33}$), voltage generating capability and sensitivity (g_{33}), charge generation capability (d_{33}) and energy conversion efficiency (k_p) was found to be on higher side for the composition $[Pb(Ni_{1/3}Sb_{2/3})]_{0.02}$–$[Pb(Zr_{0.52}Ti_{0.48})]_{0.98}O_3$ and hence can be used for power harvesting and sensors applications.

Acknowledgements

Authors would like to thank The Director, Armament Research and Development Establishment (ARDE), Pune for encouragement and permission to publish this paper. Thanks are also due to Director, Naval Materials Research Laboratory, Mumbai for extending the XRD facility. Authors also thank Director, High Energy Materials Research Laboratory, Pune for extending the SEM facility.

References

[1] G.H. Haertling, Ferroelectric ceramics: history and technology, Journal of the American Ceramic Society 82 (1999) 797–818.

[2] B. Jaffe, W.R. Cook Jr., H. Jaffe, Piezoelectric Ceramic, Academic Press, New York, 1971.

[3] H.A. Sodano, D.J. Inman, G. Park, Comparison of piezoelectric energy harvesting devices for recharging batteries, Journal of Intelligent Material Systems and Structures 16 (2005) 799–807.

[4] H.A. Sodano, D.J. Inman, G. Park, A review of power harvesting from vibration using piezoelectric, The Shock and Vibration Digest 36 (2004) 197–205.

[5] H.W. Kim, S. Priya, K. Unchino, R. Newnham, Piezoelectric energy harvesting under high pre-stressed cyclic vibrations, Journal of Electroceramics 15 (2005) 27–34.

[6] F. Mohammadi, A. Khan, R.B. Cass, Power generation from piezoelectric lead zirconate titanate fiber composites, in: Proceedings of the Material Research Society Symposium, vol. 736, 2003, pp. D5.5.1–D5.5.6.

[7] C. Green, K.M. Mossi, R.G. Bryant, Scavenging energy from piezoelectric materials for wireless sensor applications, in: Proceedings of the ASME International Mechanical Engineering Congress and Exposition, 2005.

[8] A. Mathers, K.S. Moon, Y.A. Jingang, Vibration-based PMN-PT energy harvester, IEEE Sensors Journal 9 (2009) 731–739.

[9] J.F. Tressler, A. Sedat, R. Newnham, Piezoelectric sensors and sensor materials, Journal of Electronics 2 (4) (1998) 257–271.

[10] S. Zahi, R. Bouaziz, N. Abdessalem, A dielectric and piezoelectric properties of $PbZrO_3$–$PbTiO_3$–$Pb(Ni_{1/3},Sb_{2/3})O_3$ ferroelectric ceramic system, Ceramics International 29 (2003) 35–39.

[11] C.-S. Yu, H.-L. Hsieh, Piezoelectric properties of $Pb(Ni_{1/3},Sb_{2/3})O_3$–$PbTiO_3$–$PbZrO_3$ ceramics modified with MnO_2 additive, Journal of the European Ceramic Society 25 (2005) 2425–2427.

[12] M.C. Wang, Sintering and piezoelectric properties of $Pb(Ni_{1/3}Sb_{2/3})O_3$–$PbZrO_3$–$PbTiO_3$ ceramics, Journal of Materials Science 37 (2002) 663–668.

[13] T.L. Jordan, Z. Ounaies, Piezoelectric Ceramics Characterization, ICASE Report No. 2001-28, 2001, NASA/CR-2001-211225, 2001.

[14] V. Singh, H.H. Kumar, D.K. Kharat, S. Hait, M.P. Kulkarni, Effect of lanthanum substitution on ferroelectric properties of niobium doped PZT ceramics, Materials Letters 60 (2006) 2964–2968.

[15] S.S. Chandatreya, R.M. Fulrath, J.A. Pask, Reaction mechanisms in the formation of PZT solid solutions, Journal of the American Ceramic Society 64 (1981) 422–425.

[16] R. Tipakontitikul, S. Anantha, A modified two-stage mixed oxide synthetic route to lead zirconate titanate powders, Materials Letters 58 (2004) 449–454.

[17] A. Boutarfaia, Investigations of co-existance region in lead zirconate titanate solid solutions: X-ray diffraction studies, Ceramics International 26 (2000) 583–587.

[18] R.S. Nasar, M. Cerqueira, E. Longo, J.A. Varela, A. Beltran, Experimental and theoretical study of the ferroelectric and piezoelectric behavior of strontium doped PZT, Journal of the European Ceramic Society 22 (2002) 209–218.

[19] H. Kungl, J.H. Michael, Effects of sintering temperature on microstructure and high field strain of niobium–strontium doped morphotropic lead zirconate titanate, Journal of Applied Physics 107 (2010) 054111.

[20] Ming Chen, Xi Yao, Liangying Zhang, Grain size dependence of dielectric and field-induced strain properties of chemical prepared $(Pb,La)(Zr,Sn,Ti)O_3$ antiferroelectric ceramics, Ceramic International 28 (2002) 201–207.